

HiPIMS NbN THIN FILM DEVELOPMENT FOR USE IN MULTILAYER SIS FILMS

S. Leith¹, M. Vogel¹, B. Bai¹, X. Jiang¹, E. Seiler², R. Ries²

¹Institute of Materials Engineering, University of Siegen, Siegen, Germany

²Institute of Electrical Engineering SAS, Bratislava, Slovakia

Abstract

As part of efforts to improve the performance of SRF cavities, the use of alternative structures, such as superconductor-insulator-superconductor (SIS) film coatings have been extensively investigated. Initial efforts using DC magnetron sputtering (MS) deposited NbN films showed the efficacy of this approach. The use of energetic condensation methods, such as high power impulse magnetron sputtering (HiPIMS), have already improved the performance of Nb thin films for SRF cavities and have already been used for nitride film coatings in the tool industry.

In this contribution, the results from the deposition of HiPIMS NbN thin films onto oxygen free high conductivity (OFHC) Cu substrates are presented. The effects of the different deposition parameters on the deposited films were elucidated through various characterisation methods, resulting in an optimum coating procedure. This allowed for further comparison between the HiPIMS NbN films and the previously presented DC MS NbN films. The results indicate the improvements offered by HiPIMS deposition, most notably, the significant increase in the entry field, and its applicability to the deposition of SIS films on Cu.

INTRODUCTION

Bulk Nb cavities are reaching their theoretical limits of operation. As such, new approaches are required in order to enhance the performance of future SRF cavities. One of the approaches currently being investigated is the use of superconductor-insulator-superconductor (SIS) film structures, as first proposed by A. Gurevich [1]. Initial trials of this approach have indicated its potential for enhancing the penetration field above the H_{c1} of Nb [2].

With its high T_c and high H_c , NbN stands as one of the prime candidates for use in SIS structures, even though its H_{c1} is lower than Nb [3]. One of the issues facing NbN however, is ensuring the formation of the high T_c (17.3 K [4]), δ -NbN phase. This was successfully accomplished during previous DC magnetron sputtering (MS) studies, however, the resultant film possessed a relatively low film density, resulting in decreased penetration fields compared to the theoretical value and penetration of oxygen between the NbN grains [5]. In light of this, and given the improvements offered by the use of high power impulse magnetron sputtering (HiPIMS), a series of investigations looking at the potential to deposit denser NbN films using HiPIMS were completed. The foremost aim of the investigations was to improve the field of first flux penetration (H_{en}) of the NbN films, to better serve as a shielding layer in the deposition of SIS film coatings.

The effects of the deposition parameters on the film growth, phase formation and superconducting properties were investigated in order to realise an optimum parameter set for high performance films. The results of these investigations are detailed in this contribution.

EXPERIMENTAL

A series of NbN thin films were deposited onto electropolished OFHC Cu substrates and Si witness samples with HiPIMS, using a 100.0 x 88.0 mm Nb (RRR 300) target in a commercial, high-volume, fully automated coating tool (CemeCon CC800). The HiPIMS parameters were kept constant at 1000 Hz and 120 μ s for all coatings, in conjunction with a constant DC substrate bias and a substrate temperature of 180°C. A gas mixture of Ar (99.999 Vol-%) and N₂ (99.999 Vol-%) was used for all coatings, with the N₂/Ar gas ratio maintained by flow rate control.

Prior to deposition, the system was baked at 650°C for 6 hours, to assist in removing any built up adsorbents, and thereafter evacuated to a base pressure of 6×10^{-7} mbar. The system was then backfilled with Ar to a pressure of 1.5×10^{-3} mbar for target plasma cleaning and MF etching of the substrates.

The films were deposited with a range of different deposition parameters in order to identify those that most significantly influence the NbN phase formation and subsequent superconducting performance. Based on previous experience [5], this included the cathode power, the N₂ content in the gas and the deposition pressure. With the increased ionisation ratio of the sputtered material and the resultant densification of the deposited films offered by HiPIMS, a range of substrate bias values was also included. The high and low limits of the varied parameters are detailed in Table 1.

Table 1: Set Point Ranges for the Varied Deposition Parameters Used for the NbN Film Coatings

Parameter Boundary	Cathode Power (W)	Deposition Pressure (mbar)	Substrate Bias (V)	N ₂ Content (%)
High	600	2.4×10^{-2}	100	22
Low	300	1.2×10^{-2}	0	5

Following the deposition of the films, the samples were analysed with a number of characterisation methods, including: AFM, CLSM, EDX, SEM, XRD and VSM magnetisation measurements. Specific results of interest are detailed here.

RESULTS AND DISCUSSION

The results detailed here pertain to the NbN films deposited onto the Cu substrates, except for the cross section SEM images, which were obtained for the NbN films deposited onto the Si witness samples. The average thickness of the NbN films fell within $1.28 \pm 0.12 \mu\text{m}$, with the changing deposition conditions leading to deposition rates ranging from 14.62 to 53.63 nm/min, mostly affected by the $\text{N}_2\%$ and the cathode power.

MORPHOLOGICAL AND TOPOGRAPHICAL ANALYSIS

Similar to the previously deposited DC MS films, detailed in [5], a low deposition pressure results in a dense film microstructure, albeit significantly more columnar in nature than the DC MS films. The films are topped with a smooth, rounded grain peak. This is found regardless of the cathode power or $\text{N}_2\%$. At low deposition pressures, films become increasingly nanocrystalline with increasing cathode power, due to the increased nucleation density [6]. An increase in the deposition pressure results in a slight reduction in the film density, though still largely superior to high pressure DC MS NbN films, and an increase in the columnar nature of the films, coupled to the growth of more faceted features on the film surface.

Changes in the substrate bias led to the most significant changes in the film microstructure, as presented for films deposited at 400 W and 2.2×10^{-2} mbar in Fig. 1. At 0 V substrate bias (a), the films display a disjointed columnar structure, topped by faceted peaks, similar to previous DC MS films. Increasing the substrate bias to 100 V (b) led to an increased density of the deposited film, a shift to a more nanocrystalline growth as well as rounding of the grain peaks on the film surface.

A similar behaviour is observed with an increase in the $\text{N}_2\%$, as shown in Fig. 2, where the density of the deposited films increases with increasing $\text{N}_2\%$. This is detailed for a change from 5 to 22% N_2 in Fig. 2 (a) and (b) respectively. Note that Fig. 2 (a) and (b) were deposited with 50 V substrate bias, with (b) being representative of a typical intermediate substrate bias film. Furthermore, the surface features of the films transition from faceted peaks at low $\text{N}_2\%$ to rounded features at higher $\text{N}_2\%$. This transition is delayed at lower cathode power levels, which show faceted features to a higher $\text{N}_2\%$.

Based on these observations, and the AFM results not detailed here, the surface roughness of the films are found to decrease with: increasing $\text{N}_2\%$, increasing substrate bias, increasing cathode power and decreasing deposition pressure.

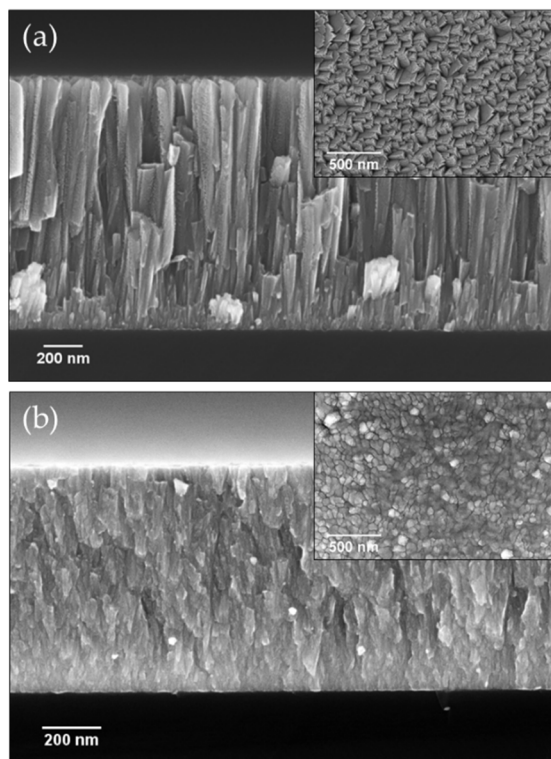


Figure 1: SEM images of samples deposited with 400 W cathode power and 2.2×10^{-2} mbar deposition pressure with different substrate bias. (a) and (b) display the films deposited with 0 and 100 V substrate bias respectively.

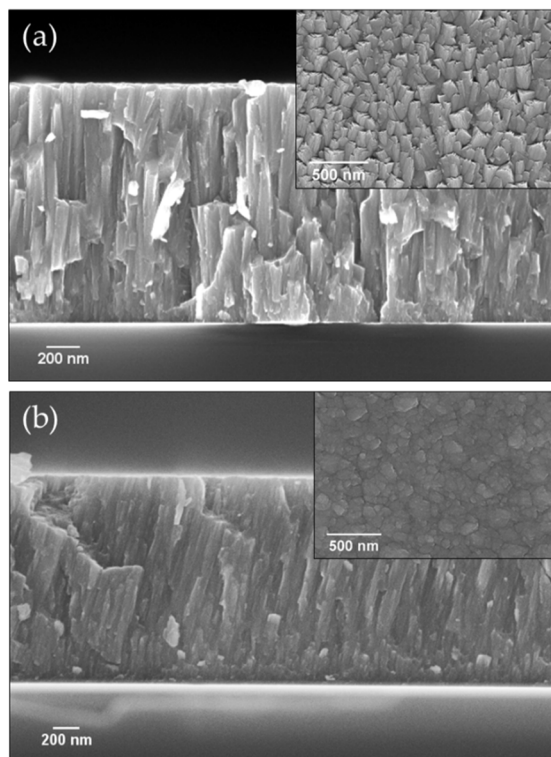


Figure 2: SEM images of samples deposited with 400 W cathode power and 2.2×10^{-2} mbar deposition pressure with different $\text{N}_2\%$. (a) and (b) display the films deposited with 5 % and 22 % N_2 respectively.

CRYSTALLOGRAPHIC ANALYSIS

Similar to DC MS NbN films, the formation of the sought after δ -NbN phase in HiPIMS-deposited NbN films is heavily reliant on the deposition pressure. Regardless of the cathode power or N_2 % used, an increase in the deposition pressure led to a transition from a hexagonal Nb_5N_6 preferred film to a cubic δ -NbN preferred film. This was generally found at pressures $> 2.0 \times 10^{-2}$ mbar. Furthermore, the transition to a cubic δ -NbN film also led to a decrease of the FWHM of the peak of highest relative intensity, indicating an increase in the crystallite size with increasing deposition pressure. Finally, for all values of N_2 % and cathode power, the out-of-plane lattice parameter decreases with increasing deposition pressure.

Figure 3 displays the XRD patterns of samples deposited at 300 W cathode power, 8% N_2 , 2.2×10^{-2} mbar and different substrate bias values. The emergence of a secondary peak at $\sim 34.5^\circ$, representative of the hexagonal Nb_5N_6 phase, is first apparent as a shoulder at a substrate bias level of 50 V. With a further increase in the substrate bias, the hexagonal phase becomes the dominant NbN phase in the film, with the δ -NbN phase disappearing completely at 100 V. The disappearance of the δ -NbN phase was apparent at higher substrate bias values regardless of changes to further deposition parameters.

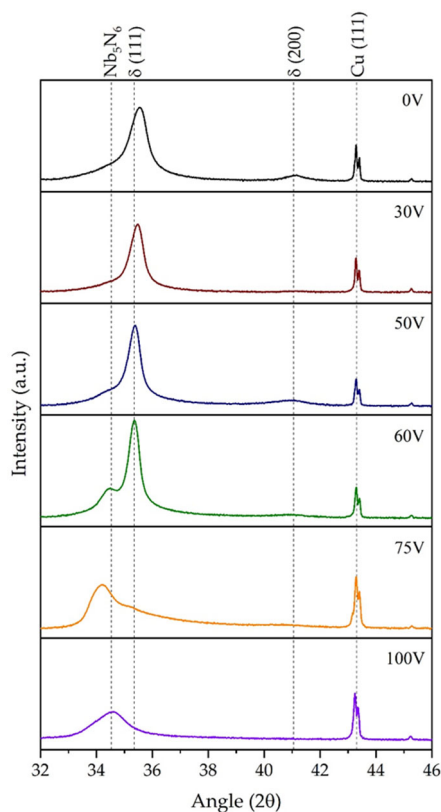


Figure 3: XRD patterns of samples deposited at 8% N_2 , 300 W cathode power, 2.2×10^{-2} mbar and different substrate bias values. The spectra are plotted in log scale.

A continuously increasing lattice parameter value was observed for increasing substrate bias levels, indicative of an increasing stress state within the film. This reaches a

maximum of 4.4229 Å at 75 V, a value greater than the reference values for bulk δ -NbN [7]. Thus, as indicated by the XRD phase analysis, substrate bias values ≥ 75 V result in a complete change in the preferred NbN phase.

The XRD spectra for samples deposited with increasing N_2 % at 2.2×10^{-2} mbar and 300 W as well as 400 W cathode power are displayed in Fig. 4 (a) and (b) respectively. Both series of samples display a gradual transition from a preferred δ -NbN (111) orientation to a preferred δ -NbN (200) orientation with increasing N_2 %. As showcased in (b), this is more pronounced for the samples deposited at 400 W. This transition is opposite to that which was observed for the DC MS NbN films. However, they were deposited at a low deposition pressure.

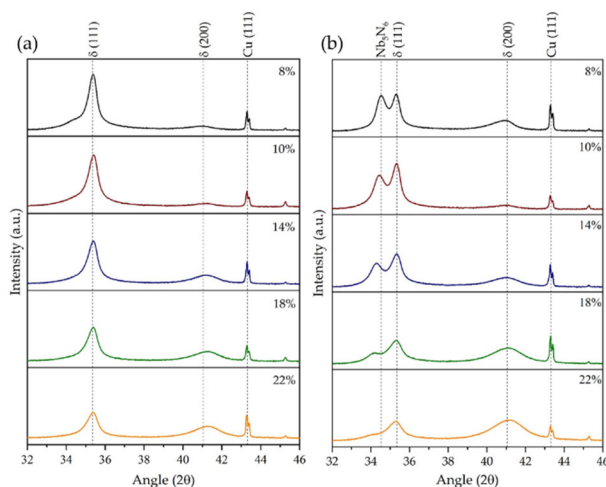


Figure 4: XRD patterns of samples deposited at different N_2 % values. The samples were deposited at a constant deposition pressure of 2.2×10^{-2} mbar and cathode powers of (a) 300 W and (b) 400 W. The spectra are plotted in log scale.

Samples deposited at 300 W do not display evidence of the hexagonal phase above 10% N_2 , whereas this peak is still visible until 22% N_2 for the samples deposited at 400 W. The increase in the proportion of cubic δ -NbN, at the expense of the hexagonal phase in the NbN films with increasing N_2 %, is similar to the results obtained for CrN films deposited with HiPIMS [8].

Based on analysis of the XRD data, it is clear that films coated at 300 W consistently display lattice parameters lower than those deposited at 400 W, with all other parameters equal, though all are within the bounds described for δ -NbN. A specific minimum in the lattice parameter values is found in the region of 10 to 15% N_2 depending on the cathode power.

On further inspection, films deposited at lower cathode power display smaller lattice parameters for all deposition pressures, likely due to the lower film stress levels because of their more disjointed microstructure, as observed in the SEM results. An increase in the N_2 % also results in a slight decrease in the lattice parameter. These results indicate a pronounced reliance on the proportion of δ -NbN within the film, with respect to its lattice parameter.

SUPERCONDUCTING ANALYSIS

The superconducting performance of NbN is very dependent on the formation of the correct stoichiometric phase, which is typically characterised by a specific lattice parameter value. For the sought after δ -NbN phase, this value theoretically lies between 4.38 – 4.42 Å [7]. The measured transition temperatures of a range of HiPIMS NbN samples, each with separately varied deposition parameters, are related to their respective out-of-plane lattice parameter values in Fig. 5. The maximum $T_c = 16.5$ K for these HiPIMS NbN films was achieved for a lattice parameter of ~ 4.396 Å, which is similar to that of the corresponding highest T_c DC MS NbN film [5]. The observed increasing trend of T_c vs. lattice parameter, up until ~ 4.40 Å, is consistent with previous work [9].

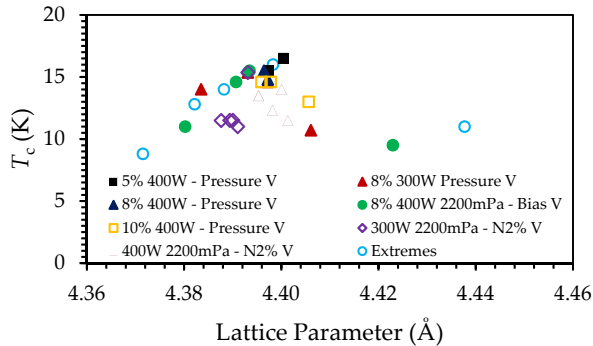


Figure 5: Plot detailing the HiPIMS NbN transition temperature as a function of the out-of-plane lattice parameter. The legend shows the constant deposition parameters while the specific variable parameter indicated by a “V”.

The T_c as well as the H_{en} , for a selection of NbN films deposited at 300 and 400 W with lower N_2 %, as a function of the deposition pressure, are detailed in Figure 6 (a). The HiPIMS NbN films show an increase in the T_c and H_{en} values with increasing deposition pressure. This correlates well with the transition to a more δ -NbN dominated film and is similar to DC MS NbN trends. Specific maximums in both T_c and H_{en} (16.5 K and 28.0 mT respectively) are observed at a deposition pressure of 2.2×10^{-2} mbar. This high H_{en} is more than double that achieved previously by DC MS, with other samples showing results of similar values.

Samples deposited with a large substrate bias value (> 75 V), showed a significant reduction in superconducting performance. At 75 V, the T_c was similar to that of bulk Nb (9.2 K), while at 100 V, no superconducting transition was observed down to 4.0 K. This was found even for samples deposited with 300 W cathode power, which typically results in the preferential formation of the δ -NbN phase. This correlates well with the phase transition detailed by the XRD data in Fig. 3.

The evolution of the T_c as well as the H_{en} of the HiPIMS NbN samples, in relation to changing N_2 %, is shown in Fig. 6 (b). Samples deposited at 400 W show a continuous decrease in T_c with increasing N_2 %. This correlates well with the gradual change in preferred orientation of the films, from δ -NbN (111) to δ -NbN (200), shown in Fig. 4

(b) and is similar to what has been observed for DC MS-deposited NbN films [5,10]. On the other hand, samples deposited at 300 W show an initial decrease in T_c , where after it remains relatively constant to higher N_2 %.

The HiPIMS NbN films showed an initial increase in H_{en} with increasing N_2 %, a marked jump at 10 % N_2 and a maximum of 30 mT at 14% (400 W), where after it decreased. This is the highest H_{en} value achieved for all NbN films and, though not corrected for geometrical factors, is in the range of the theoretical $H_{c1} = 20$ mT of NbN as well [11]. Additionally, deposition at 400 W consistently resulted in larger H_{en} values than 300 W, likely as a result of the relatively improved density of these films.

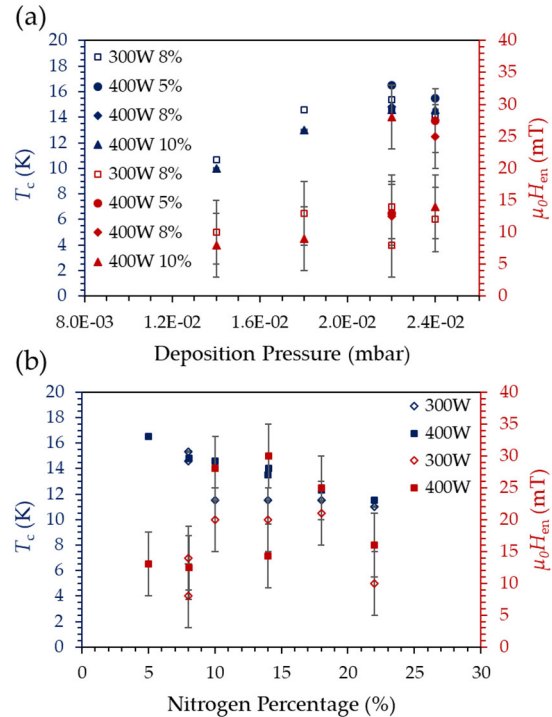


Figure 6: Plot detailing the changes in the critical temperature and the entry field of HiPIMS NbN samples, in parallel field, as a function of (a) deposition pressure and (b) N_2 %.

CONCLUSION

The results of this study indicate the significant improvements offered by the use of HiPIMS for the deposition of NbN films. Most notably, the density of the films was significantly increased while also reducing their surface roughness. A higher deposition pressure and lower cathode power were found to be more conducive to the formation of the correct δ -NbN phase. Furthermore, the use of a lower substrate bias (< 60 V) is essential, as higher substrate bias values lead to the formation of non-superconducting, hexagonal phases.

These improvements resulted in a significant increase in the entry field of these films, with most films achieving values more than the previous best obtained with DC MS. Many of the HiPIMS NbN films even achieved entry field values larger than the reported H_{c1} of bulk NbN. Interest-

ingly, the higher H_{cn} values were achieved by films characterised by a δ -NbN (111) phase as opposed to the δ -NbN (200) phase shown in high H_{cn} DC MS NbN films. Furthermore, the highest measured T_c of NbN films deposited onto Cu (16.5 K) was achieved with HiPIMS deposition.

The improved performance of these HiPIMS NbN films makes them especially applicable to SIS film coatings. The results of initial investigations into the use of HiPIMS NbN films in SIS film coatings are detailed in [12].

ACKNOWLEDGEMENTS

This work forms part of the EASITrain Marie Skłodowska-Curie Action (MSCA) Innovative Training Networks (ITN) which has received funding from the European Union's H2020 Framework Programme under Grant Agreement no. 764879.

The superconducting characterisation measurements were completed within the European Union's ARIES collaboration H2020 Research and Innovation Programme under Grant Agreement no. 730871

Part of this work was performed at the Micro- and Nanoanalytics Facility (MNAF) of the University of Siegen.

REFERENCES

- [1] A. Gurevich, "Enhancement of rf breakdown field of superconductors by multilayer coating," *Appl. Phys. Lett.*, vol. 88, no. 1, p. 012511, Jan. 2006. doi: 10.1063/1.2162264
- [2] C. Z. Antoine *et al.*, "Optimization of tailored multilayer superconductors for RF application and protection against premature vortex penetration," *Supercond. Sci. Technol.*, vol. 32, no. 8, p. 085005, Aug. 2019. doi: 10.1088/1361-6668/ab1bf1
- [3] W. M. Roach, D. B. Beringer, Z. Li, C. Clavero, and R. A. Lukaszew, "Magnetic shielding larger than the lower critical field of niobium in multilayers," *IEEE Trans. Appl. Supercond.*, vol. 23, no. 3, pp. 2012–2014, 2013. doi: 10.1109/TASC.2012.2234956
- [4] K. S. Keskar, T. Yamashita, and Y. Onodera, "Superconducting transition temperatures of RF sputtered NbN films," *Jpn. J. Appl. Phys.*, vol. 10, no. 3, pp. 370–374, 1971.
- [5] S. Leith, M. Vogel, J. Fan, E. Seiler, R. Ries, and X. Jiang, "Superconducting NbN thin films for use in superconducting radio frequency cavities," *Supercond. Sci. Technol.*, vol. 34, no. 2, p. 025006, Feb. 2021. doi: 10.1088/1361-6668/abc73b
- [6] J. A. Thornton, "Influence of apparatus geometry and deposition conditions on the structure and topography of thick sputtered coatings," *J. Vac. Sci. Technol.*, vol. 11, no. 4, pp. 666–670, Jul. 1974. doi: 10.1116/1.1312732
- [7] C. Stampfl, W. Mannstadt, R. Asahi, and A. J. Freeman, "Electronic structure and physical properties of early transition metal mononitrides: Density-functional theory LDA, GGA, and screened-exchange LDA FLAPW calculations," *Phys. Rev. B*, vol. 63, no. 15, p. 155106, Mar. 2001. doi: 10.1103/PhysRevB.63.155106
- [8] Y. P. Purandare, A. P. Ehiasarian, and P. Eh Hovsepien, "Target poisoning during CrN deposition by mixed high power impulse magnetron sputtering and unbalanced magnetron sputtering technique," *J. Vac. Sci. Technol. A*, vol. 34, no. 4, p. 041502, Jul. 2016. doi: 10.1116/1.4950886
- [9] M. R. Beebe, D. B. Beringer, M. C. Burton, K. Yang, and R. A. Lukaszew, "Stoichiometry and thickness dependence of superconducting properties of niobium nitride thin films," *J. Vac. Sci. Technol. A*, vol. 34, no. 2, p. 021510, Mar. 2016. doi: 10.1116/1.4940132
- [10] W. M. Roach, J. R. Skuza, D. B. Beringer, Z. Li, C. Clavero, and R. A. Lukaszew, "NbN thin films for superconducting radio frequency cavities," *Supercond. Sci. Technol.*, vol. 25, no. 12, p. 125016, Dec. 2012. doi: 10.1088/0953-2048/25/12/125016
- [11] A.-M. Valente-Feliciano, "Superconducting RF materials other than bulk niobium: a review," *Supercond. Sci. Technol.*, vol. 29, no. 11, p. 113002, Nov. 2016. doi: 10.1088/0953-2048/29/11/113002
- [12] S. Leith *et al.*, "The Development of HiPIMS Multilayer SIS film coatings on Copper for SRF Applications," presented at the 2021 Int. Conf. on RF Superconductivity (SRF'21), Lansing, Michigan, USA, July 2021, paper SUPFDV012, this conference.